RESEARCH ARTICLE doi.org/10.1002/adsc.70084

ADVANCED SYNTHESIS & CATALYSIS

Visible-Light-Promoted Dearomatization for The Construction of Imidazole Scaffolds

Silvia Roscales[a] and Aurelio G. Csáky[a,*]

[a] Instituto Pluridisciplinar, Universidad Complutense, Madrid 28040, Spain
E-mail: csaky@ucm.es

Manuscript received: June 9, 2025; Revised manuscript received: July 27, 2025;
Version of record online: August 21, 2025

Supporting information for this article is available on the WWW under https://doi.org/10.1002/adsc.70084

Abstract: Dearomatization is a powerful strategy for constructing complex carbocycles and heterocycles, though it typically relies on harsh conditions due to aromatic stability. Herein, a visible-light-driven photocatalytic dearomatization strategy for electron-poor imidazo[1,2-*a*]pyridines is reported, addressing a key limitation of current methods, which predominantly target electron-rich aromatic systems. Using α-keto acids as acyl radical precursors, this mild method enables the efficient synthesis of structurally diverse and functionalized imidazole derivatives, a privileged scaffold in pharmaceuticals and advanced materials. Some of the synthesized imidazoles display noteworthy photophysical properties. Some of the synthesized imidazoles show dual fluorescence from deep violet to greenish-cyan, highlighting potential as innovative fluorescent probes. This work expands the scope of dearomatization and provides a valuable tool for accessing new chemical space in drug discovery and materials science.

Keywords: C—C coupling, dearomatization, fluorescence, ketones, photocatalysis

1. Introduction

Dearomatization reactions have emerged as a powerful strategy for converting readily available aromatic precursors into partially or fully saturated, sp^3-rich frameworks.[1] These nonplanar structures expand the accessible chemical space in drug discovery, aligning with the widely recognized trend of "escape from flatland".[2] Notably, 59% of FDA-approved small-molecule drugs contain at least one nitrogen heterocycle, underscoring the importance of these motifs in medicinal chemistry.[3] Despite their prevalence, the selective saturation and functionalization of heteroarenes, particularly electron-deficient systems, remains a major synthetic challenge. In this context, dearomatization offers a cost-effective and efficient route to complex heterocyclic scaffolds with promising bioactive potential.

Several strategies have been developed over the past decade to address this issue. Traditional approaches, including Birch-type reductions under optimized conditions,[4] transition-metal-catalyzed transformations,[5] and catalytic hydrogenation,[6] have been widely explored. Most of these methods lack selectivity for sensitive substrates. More recently, visible-light-mediated dearomatization has emerged as a particularly powerful alternative.[7] By harnessing the high-energy excited states of visible-light-absorbing photocatalysts, these reactions enable the activation of heteroarenes under mild conditions, opening new avenues for selective functionalization. Unlike conventional methods, which often face limitations in installing complex functionalities, photocatalytic dearomatization allows for both skeletal editing and the introduction of diverse substituents in a single step.[8] However, current scope is limited to electron-rich aromatic systems (**Scheme 1**a).[7,9]

In search of novel, synthetically accessible scaffolds with potential relevance to drug discovery, we turned our attention to imidazo[1,2-*a*]pyridines **1**. These are "privileged" motifs widely employed in medicinal chemistry.[10] Thus far, photocatalytic strategies have only

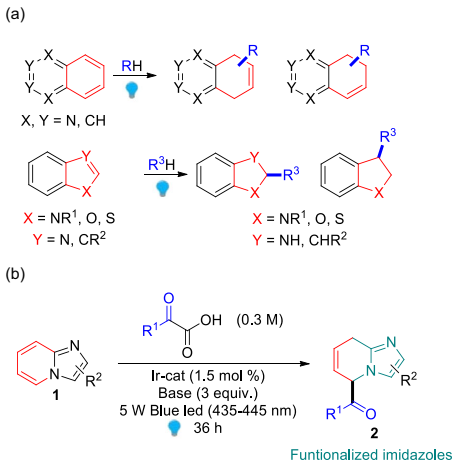

Scheme 1. Context of the current work. a) Photocatalytic dearomatization of electron-rich heteroaromatics. b) This work: Dearomatization of imidazo[1,2-*a*]pyridines.

been used for the selective C3 and C5 functionalization of imidazo[1,2-*a*]pyridines.[11] The photocatalytic dearomatization of this scaffold has not been reported.[11,12] We thus set out to develop a visible-light-driven method for the saturation of the electron-deficient pyridine moiety, providing access to the functionalized imidazoles **2** (Scheme 1b).

Functionalized imidazoles constitute a relevant class of molecules both in synthetic and medicinal chemistry.[13] In addition, imidazoles play a significant role in optical and electronic applications.[14] Their distinctive bipolar structure, comprising an electron-donating and an electron-accepting nitrogen atom separated by the C2 carbon, enhances the functional performance of chromogenic and fluorogenic derivatives. A photocatalytic dearomatization approach offers a fundamentally new and orthogonal pathway to access these valuable heterocycles under mild, operationally simple conditions.[15]

Specifically, our efforts have focused on the incorporation of acyl groups into these relevant scaffolds (Scheme 1b). Ketone derivatives are fundamental structural motifs in organic synthesis and are widely present in bioactive compounds and pharmaceuticals.[16] Their synthesis has attracted considerable attention, with radical acylation reactions emerging as one of the most efficient and versatile approaches. Acyl radicals, being inherently nucleophilic, serve as key intermediates in diverse transformations, including Giese-type additions to activated alkenes[17] and Minisci-type acylations of heteroarenes,[18] enabling access to a wide range of natural and biologically active ketones. Traditional methods for acyl radical generation often required harsh conditions such as UV irradiation or elevated temperatures, which can limit substrate scope and functional group tolerance. In contrast, the photocatalytic generation of acyl radicals under visible-light irradiation offers a mild and sustainable alternative.[19] In particular, α-keto acids can be efficiently converted into acyl radicals, enabling downstream functionalization under benign reaction conditions.[20] Their versatility as building blocks in catalytic organic synthesis further positions α-keto acids as attractive, sustainable acylating agents, providing a viable alternative to traditional acyl chlorides and other acyl-transfer reagents. α-Keto acids offer a greener alternative in organic synthesis, as they generate CO_2 as the only coproduct, making them an environmentally friendly choice.

2. Results and Discussion

We initiated our study using **1a** as the model substrate (**Scheme 2**). Initial attempts with benzoyl chloride **3** and the anhydride **4** as benzoyl radical precursors were unsuccessful: No reaction occurred with **3**, and only low yields were obtained with **4**. These results can be explained by the competitive *N*-acylation of compound **1** with either **3** or **4**. In contrast, the α-keto acid **5a** efficiently delivered product **2aa** in good yield. After optimization of the reaction conditions (see the Supporting Information for full details), **2aa** was obtained in 69% yield.

With these observations in hand, we extended the reaction to a variety of imidazo[1,2-*a*]pyridines **1** and α-keto acids **5** (**Scheme 3**). Using **5a** as the α-keto acid counterpart, a broad range of imidazo[1,2-*a*]pyridines proved to be suitable substrates for this dearomative acylation reaction (Scheme 3a). Compounds bearing a

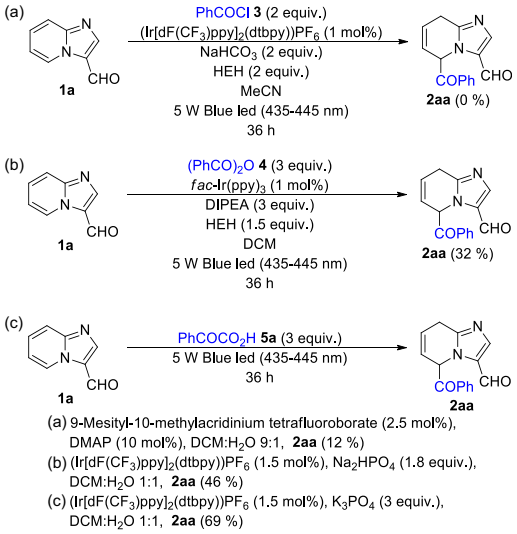

Scheme 2. Optimization of reaction conditions. a) 9-Mesityl-10-methylacridinium tetrafluoroborate (2.5 mol%), DMAP (10 mol%), DCM:H_2O 9:1, 2aa (12%). b) (Ir[dF(CF_3)ppy]$_2$(dtbpy))PF_6 (1.5 mol%), Na_2HPO_4 (1.8 equiv.), DCM:H_2O 1:1, 2aa (46%) c) (Ir[dF(CF_3)ppy]$_2$(dtbpy))PF_6(1.5 mol%), K_3PO_4 (3 equiv.), DCM:H_2O 1:1, 2aa (69%).

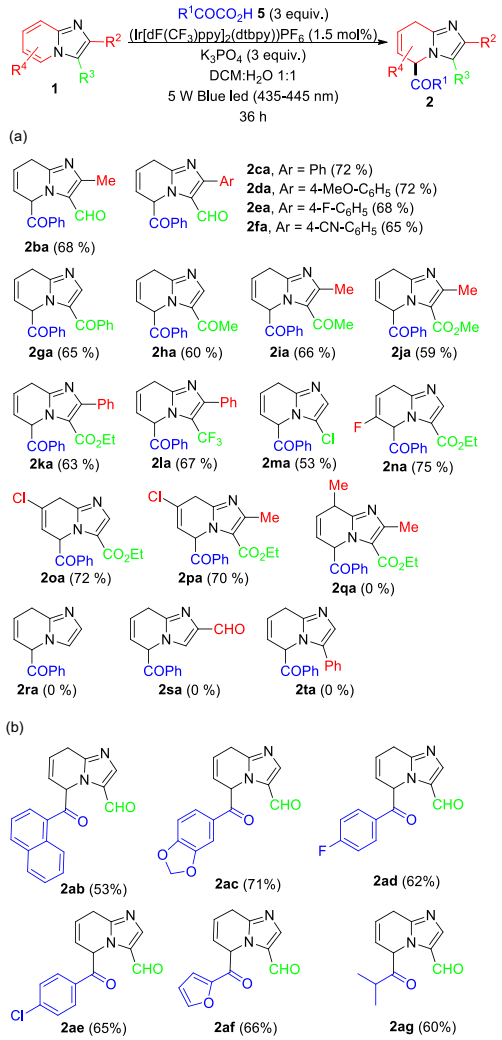

Scheme 3. Scope and limitations. a) Variation of the imidazo[1,2-*a*]pyridines 1. b) Variation of the α-keto acids 5.

3-formyl group and various substituents at C2 (R^2), either alkyl (**2ba**) or aryl (**2ca–fa**), were obtained in good yields (65–72%). Substrates with a 3-aryl (**1g**) or 3-alkyl ketone group (**1h**, **1i**) also performed well (60–66%). Similarly, 3-carboxylates bearing alkyl (**2ja**) or aryl (**2ka**) groups at position 2 were obtained in 59 and 63% yield, respectively. A 3-CF_3 substituent (**1l**) was also compatible, delivering the dearomatized product in good yield (67%). Notably, the reaction tolerated halogen substituents such as Cl, which is significant because these functional handles may enable further downstream derivatization. Moderate yields were obtained with the 3-chloro derivative **1m** (53%). Substitution by F at position 6 (**1n**, 75%) and at C7 by Cl (**1o-p**, 70–72%) led to increased yields.

A methyl substituent at C8 (**1q**) led to reduced efficiency and only traces of the desired compound **2qa** were observed. The unsubstituted imidazo[1,2-*a*]pyridine **1r**, the 2-carbaldehyde derivative **1s**, and 3-phenylimidazo[1,2-*a*]pyridine **1t** were unreactive, highlighting the essential role of an electron-withdrawing group at C3 in promoting the dearomatization reaction.

The scope of the reaction with respect to the α-keto acids **5** is shown in Scheme 3b. 2-Naphthyl-substituted glyoxylic acid **5b** proved to be a suitable acylating agent, affording product **2ab** in moderate yield. A range of 2-oxo-2-phenylacetic acids bearing either electron-donating or electron-withdrawing substituents on the aryl ring were well tolerated. Functional groups such as acetals (**5c**), aryl fluorides (**5d**), and chlorides (**5e**) were all compatible. Additionally, the 2-furyl-substituted glyoxylic acid **5f** delivered the desired product in moderate yield. Moreover, 2-isopropyl-2-oxoacetic acid (**5g**) was also reactive, and the desired product **2ag** incorporating an alkyl ketone was obtained in 60% yield.

To better understand the mechanism, we carried out a radical trapping experiment using TEMPO, which led to the formation of trapping adduct **6** in 75% yield, recovering the starting imidazo[1,2-*a*]pyridine **1a** unreactive (**Scheme 4**a). This outcome supports the involvement of a radical pathway in the reaction. Isotope-labeling studies using D_2O as solvent showed deuterium incorporation (Scheme 4b). These results support that the transformation does not proceed via a hydrogen atom transfer (HAT) mechanism.

Mechanistically, the conversion of α-keto acids to their acyl radical equivalents begins with single-electron transfer (SET) from the excited photocatalyst in its oxidated state (**[PC-Ox]***) to the α-oxocarboxylate anion, followed by decarboxylation to generate the acyl radical species (**Scheme 5**a).[19,20] These nucleophilic radicals readily add to Michael acceptors, yielding a new carbon-centered radical, which undergoes SET with the reduced photocatalyst (**[PC-Red]**). Subsequent protonation furnishes the corresponding ketone products. Building on this mechanistic basis and DFT calculations (see the Supporting Information), we propose a reaction pathway for the acylative radical dearomatization of imidazo[1,2-*a*]pyridines (Scheme 5b). Regioselective addition of the acyl radical at the C5 position of **1** generates

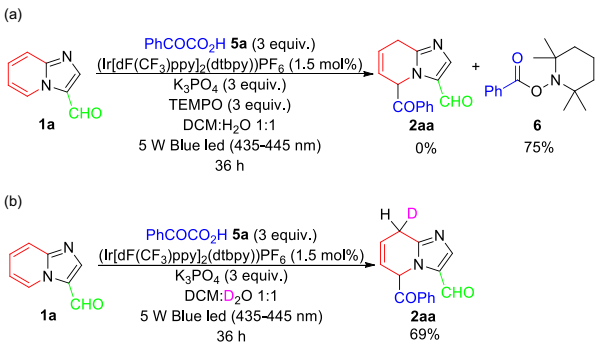

Scheme 4. Mechanistic studies. a) Radical trapping experiment. b) Isotope-labeling experiment.

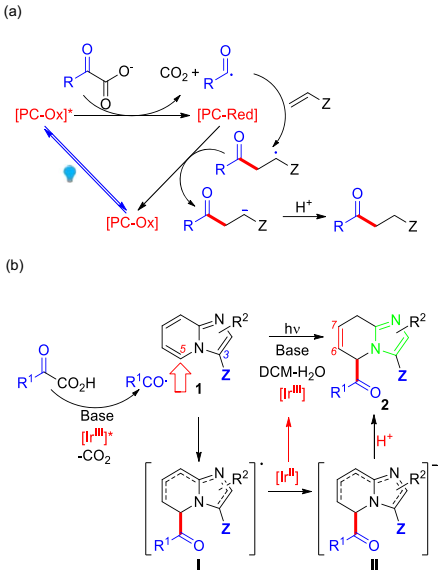

Scheme 5. Proposed reaction course. a) Photocatalyzed acyl radical addition to Michael acceptors. b) Proposed photocatalyzed acylative radical dearomatization of imidazo[1,2-*a*]pyridines.

the delocalized radical intermediate **I**. Reduction by Ir^{II} yields the delocalized anion **II**, which, upon protonation, delivers the final 5,8-dihydroimidazo[1,2-*a*]pyridine product **2** while regenerating the Ir^{III} photocatalyst. The observed regioselectivity in protonation can be rationalized by the formation of an aromatic imidazole ring and a kinetically favored Cα protonation, analogous to the behavior of dienolates, which predominantly react at the α-position rather than the γ-position.[21]

Imidazole derivatives are known for their stable photophysical properties, including high molar extinction coefficients, large Stokes shifts, high quantum yields, tunable emission wavelengths, and overall stability.[14] To explore these characteristics, the UV–vis absorption and fluorescence emission spectra of selected synthesized compounds **2** were measured in DCM and MeOH (see **Table 1** and Supporting Information). Spectral analysis revealed that the nature of substituent

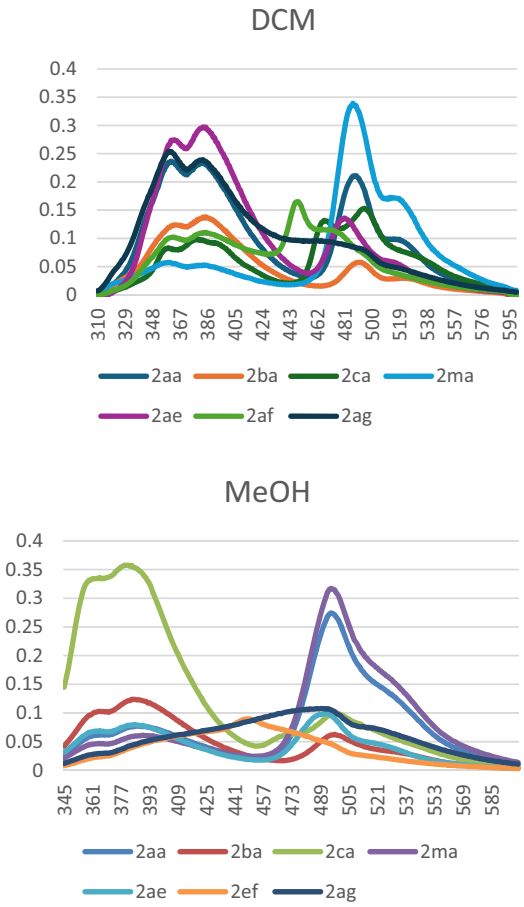

Figure 1. Fluorescence emission spectra of selected compounds recorded in DCM and MeOH.

R^3 is critical to the fluorescence behavior of these compounds, while substituents R^1 and R^2 also significantly influence emission bands and quantum yields. All compounds showed a weak absorption between 290 and 350 nm. Compounds bearing a formyl group (**2aa**, **2ba**, **2ca**, **2ae**, **2af**, **2ag**) or a chlorine atom (**2ma**) at position R^3 exhibited dual fluorescence emission in both DCM and MeOH (**Figure 1**). In DCM, two distinct

Table 1. Luminescent properties of compounds 2 in DCM and MeOH (10−4 M).

Compound[a)]	λ_{Em} [b)](DCM)	λ_{Em} [b)](MeOH)	Δ_{ss} [c)](DCM)	Δ_{ss} [c)](MeOH)	Φ[d)] (DCM)	Φ[d)] (MeOH)
2aa	383, 489	383, 495	83, 189	48, 160	0.068	0.151
2ba	385, 491	384, 497	85,191	49, 162	0.017	0.055
2ca	379, 495	381, 497	79, 195	46, 162	0.014	0.088
2ma	379, 496	389, 495	79, 196	54, 160	0.051	0.166
2ad	383, 481	385, 492	83, 181	50, 157	0.052	0.057
2af	385, 448	449	85, 148	114	0.033	0.044
2ag	383, 490	490	83, 190	155	0.110	0.115

[a)] Analysis was carried out at room temperature;
[b)] λ_{Em} = emission maxima (nm);
[c)] Δss = Stokes shifts in nm;
[d)] Φ = quantum yield.

emission bands were observed: a short-wavelength (SW) band between 359 and 385 nm, and a long-wavelength (LW) band between 481 and 495 nm, with compound **2ae** showing an emission at 448 nm. Notably, compound **2ma** (R^3 = Cl) displayed a particularly intense LW band, while in aldehyde-substituted compounds, the SW band was dominant. In MeOH, both bands persisted, but their intensities varied with the substitution pattern. For aldehydes substituted at position 2 (**2ba**, **2ca**), the SW band remained dominant, especially in compound **2ca**, which showed a strong peak at 381 nm. In contrast, compounds lacking substitution at this position (R^2 = H) showed more intense LW bands, particularly when R^1 was a Ph group (**2aa**, **2ma**). Imidazole derivatives with R^3 = ketone (**2ga**, **2ha**), ester (**2ja**, **2ka**), or CF_3 (**2la**) did not exhibit detectable fluorescence under the conditions tested.

No significant solvent polarity effect on peak positions was observed (Table 1). Stokes shifts ranged from 46 to 196 nm. Fluorescence quantum yields were measured at a concentration of 1×10^{-4} mol L^{-1} using quinine sulfate in 0.05 M H_2SO_4 ($\Phi = 0.52$) as a standard. The compounds generally showed low quantum yields in DCM (1.4–11.0%), with higher values observed in MeOH (4.4–16.6%). Overall, these findings are consistent with emission from a locally excited state (SW) and an intramolecular charge transfer (LW).

3. Conclusions

In conclusion, we have demonstrated that the electron-poor pyridine moiety of imidazo[1,2-*a*]pyridines can be dearomatized by a photocatalyzed-driven acylation reaction to furnish functionalized imidazoles. The process takes place under mild conditions, constituting a practical and operationally easy method for the synthesis of imidazole derivatives that can be particularly attractive from the standpoint of late-stage functionalization. Some of the synthesized imidazoles exhibited noteworthy photophysical properties, with several compounds showing dual fluorescence ranging from deep violet to greenish-cyan. These characteristics make them strong candidates for further development as fluorescent sensors or probes, owing to their structural tunability and distinctive dual-emission behavior. Some of the synthesized imidazoles displayed noteworthy photophysical properties, highlighting potential as innovative fluorescent probes.

4. Experimental Section

General Procedure for Photocatalized-Driven Dearomatization of Imidazo[1,2-a]pyridines: To a 10 mL vial equipped with a magnetic stir bar were added imidazo[1,2-*a*]pyridine **1** (0.2 mmol), *α*-keto acid **5** (0.6 mmol, 3 equiv), K_3PO_4 (127.4 mg, 0.6 mmol, 3 equiv), and Ir-catalyst (3.4 mg, 0.003 mmol, 1.5 mol%). The vial was sealed with a septum, and a degassed 1:1 mixture of DCM/H_2O (2 mL) was added. The reaction mixture was irradiated with a blue LED (5 W) under stirring for 36 h. Upon completion, the layers were separated, and the organic phase was dried over $MgSO_4$ and filtered. The solvent was removed under reduced pressure using a rotary evaporator. The crude residue was purified by column chromatography on silica gel to afford compounds **2**.

Supporting Information

Supporting Information is available from the Wiley Online Library or from the author.

Acknowledgements

Project PID2021-124419NB-I00 from the Spanish government (MICINN) is acknowledged for financial support.

Conflict of Interest

The authors declare no conflict of interest.

Data Availability Statement

The data that support the findings of this study are available from the corresponding author upon reasonable request.

References

[1] a) See for example: S. P. Roche, J. A. PorcoJr, *Angew. Chem. Int. Ed.* **2011**, *50*, 4068; b) W. C. Wertjes, E. H. Southgate, D. Sarlah, *Chem. Soc. Rev.* **2018**, *47*, 7996; c) C. J. Huck, D. Sarlah, *Chem* **2020**, *6*, 1589; d) N. Kratena, B. Marinic, T. J. Donohoe, *Chem. Sci.* **2022**, *13*, 14213; e) M. Escolano, D. Gaviña, G. Alzuet-Piña, S. Díaz-Oltra, M. Sánchez-Roselló, C. del Pozo, *Chem. Rev.* **2024**, *124*, 1122.

[2] a) F. Lovering, J. Bikker, C. Humblet, *J. Med. Chem.* **2009**, *52*, 6752; b) F. Lovering, *Med. Chem. Commun.* **2013**, *4*, 515.

[3] E. Vitaku, D. T. Smith, J. T. Njardarson, *J. Med. Chem.* **2014**, *57*, 10257.

[4] a) For Recent Examples, See: P. Lei, Y. Ding, X. Zhang, A. Adijiang, H. Li, Y. Ling, J. An, *Org. Lett.* **2018**, *20*, 3439; b) J. P. Cole, D. F. Chen, M. Kudisch, R. M. Pearson, C. H. Lim, G. M. Miyake, *J. Am. Chem. Soc.* **2020**, *142*, 13573; c) J. Burrows, S. Kamo, K. Koide, *Science* **2021**, *374*, 741; d) Y. Gao, K. Kubota, H. Ito, *Angew. Chem. Int. Ed.* **2023**, *62*, e202217723.

[5] a) For Recent Examples, See: A. R. Pape, K. P. Kaliappan, E. P. Kündig, *Chem. Rev.* **2000**, *100*, 2917; b) R. Gunasekar, R. L. Goodyear, I. P. Silvestri, J. Xiao, *Org. Biomol. Chem.* **2022**, *20*, 1794.

[6] a) For Recent Examples, See: M. P. Wiesenfeldt, Z. Nairoukh, T. Dalton, F. Glorius, *Angew. Chem. Int. Ed.* **2019**, *58*, 10460; b) A. N. Kim, B. M. Stoltz, *ACS Catal.* **2020**, *10*, 13834; c) R. Gunasekar, R. L. Goodyear, I. P. Silvestri, J. Xiao, *Org. Biomol. Chem.* **2022**, *20*, 1794; d) L. Lückemeier, M. Pierau, F. Glorius, *Chem. Soc. Rev.* **2023**, *52*, 4996.

[7] a) For Recent Reviews, See: Y.-Z. Cheng, Z. Feng, X. Zhang, S.-L. You, *Chem. Soc. Rev.* **2022**, *51*, 2145; b) P. Ji, K. Duan, M. Li, Z. Wang, X. Meng, Y. Zhang, W. Wang, *Chem. Soc. Rev.* **2024**, *53*, 6600, and references cited therein.

[8] a) G. E. M. Crisenza, P. Melchiorre, *Nat. Commun.* **2020**, *11*, 803; b) J. D. Bell, J. A. Murphy, *Chem. Soc. Rev.* **2021**, *50*, 9540.

[9] a) E. Y. K. Tan, A. S. M. Lani, W. Sow, Y. Liu, H. Li, S. Chiba, *Angew. Chem. Int. Ed.* **2023**, *62*, e202309764; b) M. Mikhael, S. N. Alektiar, C. S. Yeung, Z. K. Wickens, *Angew. Chem. Int. Ed.* **2023**, *62*, e202303264; c) E. Montinho-Inacio, D. Bouchet, W.-Y. Ma, P. Retailleau, L. Neuville, G. Masson, *Eur. J. Org. Chem.* **2024**, *27*, e202400248.

[10] a) See for Example: B. O. Sucu, *Med. Chem. Res.* **2022**, *31*, 2231; b) A. M. H. Altaher, M. A. Adris, S. H. Aliwaini, *Sys. Rev. Pharm.* **2021**, *12*, 79; c) R. Goel, V. Luxami, K. Paul, *Curr. Top. Med. Chem.* **2016**, *16*, 3590; d) N. Devi, D. Singh, R. K. Rawal, J. Bariwal, V. Singh, *Curr. Top. Med. Chem.* **2016**, *16*, 2963; e) A. Deep, R. Bhatia, R. Kaur, S. Kumar, U. Jain, H. Singh, S. Kaushik, P. Deb, *Curr. Med. Chem.* **2016**, *17*, 238; f) C. Enguehard-Gueiffier, A. Gueiffier, *Mini-Rev. Med. Chem.* **2007**, *7*, 888.

[11] a) C.-H. Ma, M. Chen, Z.-W. Feng, Y. Zhang, J. Wang, Y.-Q. Jiang, B. Yu, *New J. Chem.* **2021**, *45*, 9302; b) Z. Tashrifi, M. Mohammadi-Khanaposhtani, B. Larijani, M. Mahdavi, *Eur. J. Org. Chem.* **2020**, *269*, 269; c) A. B. Gadekar, V. N. S. Sonam, K. R. Bhawani, A. Kumar, *Adv. Synth. Catal* **2024**, *366*, 4794; d) S. Jin, B. Xie, S. Lin, C. Min, R. Deng, Z. Yan, *Org. Lett.* **2019**, *21*, 3436; e) Z.-Q. Zhu, D. Guo, J.-J. Ji, X. Zhu, J. Tang, Z.-B. Xie, Z.-G. Le, *J. Org. Chem.* **2020**, *85*, 15062; f) J.-J. Ji, Z.-Q. Zhu, L.-J. Xiao, D. Guo, X. Zhu, J. Tang, J. Wu, Z.-B. Xie, Z.-G. Le, *Org. Chem. Front.* **2019**, *6*, 3693.

[12] a) For Reviews, See: O. P. S. Patel, N. K. Nandwana, L. J. Legoabe, B. C. Das, A. Kumar, *Adv. Synth. Catal.* **2020**, *362*, 4226; b) A. K. Bagdi, A. Hajra, *Org. Biomol. Chem.* **2020**, *18*, 2611.

[13] a) See for for Example: N. Rani, R. Singh, P. Kumar, *Curr. Org. Synth.* **2023**, *20*, 630; b) A. Siwach, P. K. Verma, *BMC Chem.* **2021**, *15*, 12; c) P. Sharma, C. LaRosa, J. Antwi, R. Govindarajan, K. A. Werbovetz, *Molecules* **2021**, *26*, 4213; d) S. S. Alghamdi, R. S. Suliman, K. Almutairi, K. Kahtani, D. Aljatli, P. Teli, *Drug Des. Devel. Ther* **2021**, *15*, 3289; e) P. Teli, N. Sahiba, A. Sethiya, J. Soni, in *Imidazole derivatives: Impact and prospects in antiviral drug discovery* (Ed. S. Agarwal) *Imidazole-Based Drug Discovery* **2022**, pp. 167–193, Ch. 4, https://doi.org/10.1016/B978-0-323-85479-5.00001-0.

[14] a) See for Example: K. Kumar, D. Thakur, *Soft Matter* **2024**, *20*, 1669; b) O. F. A. Sharif, L. M. Nhari, R. M. El-Shishtawy, A. M. Asiri, *Mater. Today Chem.* **2023**, *29*, 101453.

[15] a) C. J. Lovely, Y. Chen, E. V. Ekanayake, *Heterocycles* **2007**, *74*, 873; b) Y. Chen, H. V. R. Dias, C. J. Lovely, *Tetrahedron Lett.* **2003**, *44*, 1379; c) Y. Matsuda, H. Gotou, K. Katou, H. Matsumoto, M. Yamashita, Y. Abe, Y. Oikawa, M. Yamaguchi, K. Torisu, *Heterocycles* **1991**, *32*, 2217.

[16] a) See for Example: D. J. Foley, H. Waldmann, *Chem. Soc. Rev.* **2022**, *51*, 4094; b) M. Blangetti, H. Rosso, C. Prandi, A. Deagostino, P. Venturello, *Molecules* **2013**, *18*, 1188; c) J. Otera, in *Modern Carbonyl Chemistry*, Wiley-VCH, Weinheim, **2000**; d) N. J. Lawrence, *J. Chem. Soc., Perkin Trans. 1* **1998**, *1739*, 1739.

[17] A. L. G. Kanegusuku, J. L. Roizen, *Angew. Chem. Int. Ed.* **2021**, *60*, 21116.

[18] a) S. Pillitteri, E. V. Van der Eycken, U. K. Sharma, *Chem. Commun.* **2025**, *61*, 13; b) X. Zhang, S. Li, F. Qiu, H. T. Ang, J. Wu, P. Jia, *Green Chem.* **2024**, *26*, 3595.

[19] a) See for Example: N. Chalotra, S. Sultan, B. A. Shah, *Asian J. Org. Chem.* **2020**, *9*, 863; b) A. Banerjee, Z. Lei, M.-Y. Ngai, *Synthesis* **2019**, *51*, 303.

[20] a) For Recent Examples, See: A. M. Davies, S. S. Londhe, E. R. Smith, J. A. Tunge, *Org. Lett.* **2023**, *25*, 8634; b) B. Ma, Y. Gong, Y. Long, Z. Chen, Y. Yuan, J. Yang, *J. Org. Chem.* **2024**, *89*, 1669; c) H.-L. Zhu, F.-L. Zeng, X.-L. Chen, K. Sun, H.-C. Li, X.-Y. Yuan, L.-B. Qu, B. Yu, *Org. Lett.* **2021**, *23*, 2976; d) F. Penteado, E. F. Lopes, D. Alves, G. Perin, R. G. Jacob, E. J. Lenardão, *Chem. Rev.* **2019**, *119*, 7113; e) D.-L. Zhu, Q. Wu, D. J. Young, H. Wang, Z.-G. Ren, H.-X. Li, *Org. Lett.* **2020**, *22*, 6832; f) L.-N. Guo, H. Wang, X.-H. Duan, *Org. Biomol. Chem.* **2016**, *14*, 7380; g) J. Schwarz, B. König, *Green Chem.* **2018**, *20*, 323.

[21] M. Oiarbide, C. Palomo, *Chem. Eur. J.* **2021**, *27*, 10226.